

Supporting Information

Photo-Induced Electron Transfer Between a Noble-Metal-Free [Mo₆I₈Cl₆]²⁻ Cluster-Based Complex and Polyoxometalates

Anam Fatima,^a Yevheniia Smortsova,^a Clément Falaise,^{*b} Nathalie Leclerc,^b Mohamed Haouas,^b Emmanuel Cadot,^b Stéphane Cordier,^c Yann Molard,^c Thomas Pino,^a Céline Dablemont,^a Rachel Méallet,^{*a} Karine Steenkeste,^{*a} Minh-Huong Ha-Thi^{*a}

- a. ISMO-CNRS UMR 8214, Université Paris-Saclay; Rue André Rivière 91400 Orsay (France).
- b. ILV-CNRS UMR 8180, UVSQ, Université Paris-Saclay; 45 Avenue des Etats Unis, 78035 Versailles Cedex (France)
- c. Institut des Sciences Chimiques de Rennes, UMR 6226 CNRS, Université de Rennes 1; Avenue du General Leclerc, 35042 Rennes (France)

Outline

1. Materials and Methods	4
a. Synthesis of cluster and polyoxometalates	4
b. Preparation of samples	5
c. Steady-state absorption and fluorescence spectroscopy	5
d. Time-resolved emission spectroscopy	6
e. Transient absorption spectroscopy	6
f. Electrochemical measurements	6
2. Supporting data	7
Figure S1. Emission spectrum of $[\text{Mo}_6\text{I}_8\text{Cl}_6]^{2-}$ in deaerated acetonitrile, $\lambda_{\text{exc}} = 420 \text{ nm}$	7
Figure S2. Emission spectra of $[\text{Mo}_6\text{I}_8\text{Cl}_6]^{2-}$ powder at different temperatures from 268 to 80 K, $\lambda_{\text{exc}} = 375 \text{ nm}$	7
Figure S3. Time-resolved emission spectra of $[\text{Mo}_6\text{I}_8\text{Cl}_6]^{2-}$ detailed at indicated delay times ($\lambda_{\text{exc}} = 420 \text{ nm}$, 20 mW) in deaerated acetonitrile. The inset shows the monoexponential fit of the kinetics at the maximum of the emission	8
Figure S4. Time-resolved emission spectra detailed of $[\text{Mo}_6\text{I}_8\text{Cl}_6]^{2-}$ at different delays between pump ($\lambda_{\text{exc}} = 420 \text{ nm}$, 20 mW) and probe in aerated acetonitrile. The inset shows the monoexponential fit of the kinetics at 700 nm	8
Figure S5. Stern-Volmer plots comparing the quenching efficiencies of the four POMs under study obtained from emission intensity of $\text{TBA}_2[\text{Mo}_6\text{I}_8\text{Cl}_6]$ cluster excited state in deaerated acetonitrile	9
Table S1. Summary of emission quenching rate constants (k_q) obtained by the Stern-Volmer analysis of the emission intensities in the presence of different POMs.	9
Figure S6. (A) Steady state emission spectra (corrected for POM absorption), and (B) time resolved emission decays of $[\text{Mo}_6\text{I}_8\text{Cl}_6]^{2-}$ - $[\text{SiW}_{12}\text{O}_{40}]^{4-}$ pair showing quenching of the cluster in deaerated acetonitrile, $\lambda_{\text{exc}} = 420 \text{ nm}$	10
Figure S7. (A) Steady state emission spectra (corrected for POM absorption), and (B) time resolved emission decays of $[\text{Mo}_6\text{I}_8\text{Cl}_6]^{2-}$ - $[\text{P}_2\text{W}_{18}\text{O}_{62}]^{6-}$ pair showing quenching of the cluster in deaerated acetonitrile, $\lambda_{\text{exc}} = 420 \text{ nm}$	10
Figure S8. (A) Steady state emission spectra (corrected for POM absorption), and (B) time resolved emission decays of $[\text{Mo}_6\text{I}_8\text{Cl}_6]^{2-}$ - $[\text{BW}_{12}\text{O}_{40}]^{5-}$ pair showing quenching of the cluster in deaerated acetonitrile, $\lambda_{\text{exc}} = 420 \text{ nm}$	11
Figure S9. (TOP) Cyclic voltammograms of polyoxometalate anions in anhydrous and deaerated acetonitrile with 0.1 M TBA.PF_6 . Reference electrode: Ag wire; Working electrode: glassy carbon; and Auxiliary electrode: Carbon. The TBA salts of POMs ($[\text{H}_2\text{W}_{12}\text{O}_{40}]^{6-}$ $[\text{P}_2\text{W}_{18}\text{O}_{62}]^{6-}$) showed distorted ill-defined waves in CH_3CN due to the presence of protons. On the addition of about 1 eq. of TBA.OH per POM, the ill-defined waves disappeared completely, leaving a two-step redox wave. (BOTTOM) Cyclic voltammograms of isocharged POMs in anhydrous and deaerated acetonitrile with 0.1 M TBA.PF_6 . Reference electrode: Ag wire; Working electrode: glassy carbon; and Auxiliary electrode: Carbon	12

Figure S10. Cyclic voltammogram of $\text{Na}_2[\text{Mo}_6\text{I}_8\text{Cl}_6]^{2-}$ in deoxygenated water with 2 Meq. of cyclodextrin. Reference electrode: Ag wire; Working electrode: glassy carbon; and Auxiliary electrode: Carbon.....	13
Figure S11. (a) Steady-state and (b) time-resolved emission quenching of the cluster by $[\text{PW}_{11}\text{VO}_{40}]^{4-}$ in deaerated acetonitrile, $\lambda_{\text{exc}} = 420 \text{ nm}$	13
Figure S12. (a) Steady-state and (b) time-resolved emission quenching of the cluster by $[\text{SiW}_{11}\text{MoO}_{40}]^{4-}$ in deaerated acetonitrile, $\lambda_{\text{exc}} = 420 \text{ nm}$	14
Figure S13. (a) Steady-state and (b) time-resolved emission quenching of the cluster by $[\text{SiMo}_{12}\text{O}_{40}]^{4-}$ in deaerated acetonitrile, $\lambda_{\text{exc}} = 420 \text{ nm}$	14
Figure S14. (a) Emission intensity and (b) lifetime Stern-Volmer plots for the three cluster-POM pairs.....	14
Figure S15. Decay associated difference spectra (DADS) of cluster- $[\text{PW}_{12}\text{O}_{40}]^{3-}$ obtained by global fitting of TA kinetics.....	15
Figure S16. Spectro-electrochemical difference spectra of quantitatively oxidized molybdenum halide cluster	15
Figure S17. Spectro-electrochemical difference spectra of quantitatively one-electron reduced polyoxometalate anions (A) $[\text{PW}_{12}\text{O}_{40}]^{3-}$, and (B) $[\text{P}_2\text{W}_{18}\text{O}_{62}]^{6-}$ in acetonitrile.....	15
Figure S18. (A) TA spectra along with the kinetic fit at 520 nm shown in the inset and (B) decay associated difference spectra (DADS) of cluster (60 μM)- $[\text{BW}_{12}\text{O}_{40}]^{5-}$ (300 μM) POM pair obtained by global fitting of TA kinetics ($\lambda_{\text{exc}} = 420 \text{ nm}$, 20 mW).	16
Figure S19. (A) TA spectra along with the kinetic fit at 520 nm shown in the inset and (B) decay associated difference spectra (DADS) of cluster (60 μM)- $[\text{H}_2\text{W}_{12}\text{O}_{40}]^{6-}$ (300 μM) POM pair obtained by global fitting of TA kinetics ($\lambda_{\text{exc}} = 420 \text{ nm}$, 20 mW)	16
Figure S20. Decay associated difference spectra (DADS) of cluster- $[\text{P}_2\text{W}_{18}\text{O}_{62}]^{6-}$ POM pair obtained by global fitting of TA kinetics.....	17
3. Author contributions	17
4. References	17

1. Materials and Methods

a. Synthesis of cluster and polyoxometalates

Chemicals and solvents for all synthesis and characterization procedures were purchased from chemPUR, Sigma-Aldrich, and TCI, and are used as it is.

$(\text{TBA})_2[\text{Mo}_6\text{I}_8\text{Cl}_6]$, $\text{H}_3[\text{PW}_{12}\text{O}_{40}] \cdot 14\text{H}_2\text{O}$, $\text{Na}_{0.6}\text{H}_{3.4}[\text{SiW}_{12}\text{O}_{40}] \cdot 16\text{H}_2\text{O}$, $\text{K}_{4.3}\text{Na}_{0.7}[\text{BW}_{12}\text{O}_{40}] \cdot 17\text{H}_2\text{O}$, and $\text{Rb}_6[\text{H}_2\text{W}_{12}\text{O}_{40}] \cdot 11\text{H}_2\text{O}$, $\text{K}_6[\text{P}_2\text{W}_{18}\text{O}_{62}] \cdot 19\text{H}_2\text{O}$, $\text{TBA}_4[\text{SiW}_{11}\text{MoO}_{40}]$, $\text{TBA}_4[\text{SiMo}_{12}\text{O}_{40}]$ and $\text{Na}_1\text{K}_3[\text{PW}_{11}\text{VO}_{40}] \cdot 7\text{H}_2\text{O}$ were prepared according to literature procedures and checked by routine analyses (IR, TGA, EDX, and NMR).¹⁻⁸ The protonation degree have been determined based on TGA analysis.

The TBA salts of POM have been prepared by metathesis process as described below.

Preparation of $\text{TBA}_3[\text{PW}_{12}\text{O}_{40}]$. $\text{H}_3[\text{PW}_{12}\text{O}_{40}] \cdot 14\text{H}_2\text{O}$ (5 g, 1.6 mmol) was suspended in 40 mL of H_2O . In a separate beaker, tetrabutylammonium bromide (5 g, 15.5 mmol) was dissolved in 50 mL of distilled water. This resulting solution was added to the $[\text{PW}_{12}\text{O}_{40}]^{3-}$ solution, leading to the precipitation of a white solid. After gentle stirring for 30 min at room temperature, the solid was collected by filtration through a fine frit, then washed with water (100 mL), ethanol (20 mL), and dried with diethyl ether (20 mL). Yield > 85 %. IR spectrum: 799 (s), 891 (s), 955 (m), 971 (m), 1008 (m), 1487 (s), 2360 (m), 2880 (s), 2950 (w), 2970 (s) cm^{-1} .

Preparation of $\text{TBA}_4[\text{SiW}_{12}\text{O}_{40}]$. $\text{Na}_{0.6}\text{H}_{3.4}[\text{SiW}_{12}\text{O}_{40}] \cdot 16\text{H}_2\text{O}$ (5 g, 1.54 mmol) was suspended in 40 mL of H_2O . In a separate beaker, tetrabutylammonium bromide (5 g, 15.5 mmol) was dissolved in 50 mL of distilled water. This resulting solution was added to the $[\text{SiW}_{12}\text{O}_{40}]^{4-}$ solution, leading to the precipitation of a white solid. After gentle stirring for 30 min at room temperature, the solid was collected by filtration through a fine frit, then washed with water (100 mL), ethanol (20 mL), and dried with diethyl ether (20 mL). Yield > 85 %. IR spectrum: 784 (s), 875 (s), 920 (m), 974 (m), 1011 (m), 1487 (s), 2360 (m), 2880 (s), 2950 (w), 2970 (s) cm^{-1} .

Preparation of $\text{TBA}_5[\text{BW}_{12}\text{O}_{40}]$. $\text{K}_{4.3}\text{Na}_{0.7}[\text{BW}_{12}\text{O}_{40}] \cdot 17\text{H}_2\text{O}$ (5 g, 1.5 mmol) was suspended in 40 mL of H_2O . The dodecatungstoboric acid has been prepared by passage of this aqueous solution through a column of Dowex 50WX8 (H^+ form). Then, the resulting colorless solution of $\text{H}_5[\text{BW}_{12}\text{O}_{40}]$ has been added to a 250 mL solution of tetrabutylammonium bromide (0.3 M). After stirring for 30 min at room temperature, the white solid was collected by filtration through a fine frit, then washed with water (100 mL), ethanol (20 mL), and dried with diethyl ether (20 mL). Yield > 85 %. IR spectrum: 800 (s), 892 (s), 946 (s), 989 (w), 1489 (s), 2360 (m), 2887 (s), 2950 (w), 2960 (s) cm^{-1} .

Preparation of $\text{TBA}_{4.8}\text{H}_{1.2}[\text{H}_2\text{W}_{12}\text{O}_{40}]$. $\text{Rb}_6[\text{H}_2\text{W}_{12}\text{O}_{40}] \cdot 11\text{H}_2\text{O}$ (5 g, 1.4 mmol) was suspended in 40 mL of H_2O . The metatungstic acid has been prepared by passage of this solution through a column of Dowex 50WX8 (H^+ form). Then, the resulting colorless solution of $\text{H}_6[\text{H}_2\text{W}_{12}\text{O}_{40}]$ has been added to a 250 mL solution of tetrabutylammonium bromide (0.3 M). After stirring for 30 min at room temperature, the white solid was collected by filtration through a fine frit, then washed with water (100 mL), ethanol (20 mL), and dried with diethyl ether (20 mL). Yield > 85 %. IR spectrum: 705 (w), 792 (s), 885 (s), 953 (s), 1480 (s), 2870 (s), 2950 (w), 2960 (s) cm^{-1} .

Preparation of $\text{TBA}_{5.5}\text{H}_{0.5}[\text{P}_2\text{W}_{18}\text{O}_{62}]$. $\text{K}_6[\text{P}_2\text{W}_{18}\text{O}_{62}] \cdot 19\text{H}_2\text{O}$ (5 g, 1 mmol) was suspended in 40 mL of H_2O . Acid salt of $[\text{P}_2\text{W}_{18}\text{O}_{62}]^{6-}$ has been prepared by passage of this aqueous solution through a column of Dowex 50WX8 (H^+ form). Then, the resulting colorless solution of POMs has been added to a 75 mL solution of tetrabutylammonium bromide (0.3 M). After stirring for 30 min at room

temperature, the white solid was collected by filtration through a fine frit, then washed with water (100 mL), ethanol (20 mL), and dried with diethyl ether (20 mL). Yield > 85 %. IR spectrum: 785 (w), 911 (s), 956 (s), 1090 (s), 1480 (s), 2870 (s), 2950 (w), 2960 (s) cm^{-1} .

Preparation of $\text{TBA}_4[\text{PW}_{11}\text{VO}_{40}]$. $\text{H}_4[\text{PW}_{11}\text{VO}_{40}] \cdot 15\text{H}_2\text{O}$ (5 g, 1.65 mmol) was suspended in 40 mL of H_2O . In a separate beaker, tetrabutylammonium bromide (5 g, 15.5 mmol) was dissolved in 50 mL of distilled water. This resulting solution was added to the yellow solution of $[\text{PW}_{11}\text{VO}_{40}]^{4-}$, leading to the precipitation of a yellowish solid. After gentle stirring for 30 min at room temperature, the solid was collected by filtration through a fine frit, then washed with water (100 mL), ethanol (20 mL), and dried with diethyl ether (20 mL). Yield > 85 %.

Preparation of $\text{TBA}_4[\text{SiW}_{11}\text{MoO}_{40}]$. $\text{K}_4[\text{SiW}_{11}\text{MoO}_{40}] \cdot 16\text{H}_2\text{O}$ (5 g, 1.55 mmol) was dissolved in 30 mL of water and then precipitated with tetrabutylammonium bromide (5 g, 15.5 mmol). The resulting yellow salt collected by filtration through a fine frit, and washed with water and dried with diethyl ether (20 mL). Yield > 85 %.

Preparation of $\text{TBA}_4[\text{SiMo}_{12}\text{O}_{40}]$. A concentrated nitric acid (13M, 12.3 mL) was added to a solution prepared from sodium molybdate (1M, 40 mL) and metasilicate (0.2M, 16.6 mL). This yellow solution is heated at 80°C during 1 hour. Then tetrabutylammonium bromide (3 g, 9.3 mmol) was added to this solution. The resulting yellow salt was collected by filtration through a fine frit, washed with water, ethanol, and diethyl ether. Recrystallization in acetone yielded small yellow needles. Yield > 80 %.

b. Preparation of samples

Photophysical studies. To prevent the oxygen quenching of the cluster $[\text{Mo}_6\text{I}_8\text{Cl}_6]^{2-}$, all the sample solutions were recorded under oxygen-free conditions. First, the solvent was purged with argon for 30 min and then the samples were prepared inside the glovebox with the argon-saturated solvent.

Measurement of the UV-vis spectrum of one-electron reduced POMs. Each one-electron reduced POM has been prepared under argon using bulk electrolysis in acetonitrile containing $n\text{Bu}_4\text{N} \cdot \text{PF}_6$ (0.1 M) as supporting electrolyte. To reduce the POM compounds, the chronoamperometry were performed at potential corresponding to about 120 mV below the half-wave potential of the first redox event. The reduction of the POMs led to the formation of blue solutions. To avoid the reoxidation by air (very fast process), we systematically handled the solutions under inert atmosphere.

Measurement of the UV-vis spectrum of one-electron oxidized cluster. The oxidation of the molybdenum halide cluster $[\text{Mo}_6\text{I}_8\text{Cl}_6]^-$ by bulk electrolysis under argon in acetonitrile led to formation of insoluble precipitate at the working electrode interface. This phenomenon has been previously observed by Efremova and coworkers.¹ To tackle this problem, we performed the oxidation of the cluster $\text{Na}_2[\text{Mo}_6\text{I}_8\text{Cl}_6]$ (2 mM) in 25 mM HClO_4 aqueous solution containing γ -cyclodextrin (4 mM). The use of cyclodextrin is required to stabilize the cluster in water, the CD host avoids the hydrolysis of the terminal chloride ligands.⁹ In such conditions, the metal atom cluster exhibits a reversible oxidation at +1 V vs SCE.² The controlled potential oxidation has been performed by applying the potential at +1.1 V vs SCE. During the oxidization of the cluster, the solution turned olive green (see Figure S16), and the process was monitored by steady-state voltammetry using rotating disk electrode to verify the completion of the one-electron oxidation.

c. Steady-state absorption and fluorescence spectroscopy

UV-vis ground state absorption spectroscopy was performed on a UV-2600 spectrophotometer from Shimadzu. The sample concentrations used for absorption and emission measurements were in the micro-molar range, and the spectra were recorded in standard quartz cuvettes with a 1 cm optical path.

Emission spectra were measured with Scientific Fluoromax PLUS (Horiba Jobin-Yvon) at room temperature in deaerated acetonitrile solution. The presented emission spectra are corrected for the response of the emission monochromator and the detector. All samples were excited at 420 nm with an excitation and emission slit band pass of 2 nm, in both cases.

d. Time-resolved emission spectroscopy

The excitation light source for the time-resolved emission measurements is based on a Nd:YAG Laser (EKSPLA) yielding 4 ns pulses with a repetition rate of 10 Hz. After passing through the sample, the emission light was sent to the spectrograph (SPEX 270M, Jobin-Yvon) via a bundle of optical fiber for analysis. The dispersed light from the spectrograph is then detected by an intensified charge coupled device (ICCD) camera, PIMAX-4 (Princeton Instrument). The obtained spectra were not corrected by the sensitivity of the spectrometer. The emission kinetics were studied between 400 and 700 nm.

e. Transient absorption spectroscopy

To excite the samples for laser flash photolysis, an optical parametric oscillator (OPO) pumped by a pulsed nanosecond Nd:YAG laser (EKSPLA) was used. The pump laser operates at a frequency of 10 Hz. The resulting pulse width was 4 ns, with an energy of 1-2 mJ/pulse. For transient absorption measurements, a nanosecond white light super continuum laser (STM-2-UV LEUKOS, temporal width of < 1 ns) was used as a probe light. The probe laser was set to a repetition rate of 20 Hz. To monitor spectral energy distribution fluctuations, the probe beam was split by a beam splitter, which directed one part of the beam to the sample cell and the other to the reference. The sample's transmitted light enters the center of the optical fiber (round-to-linear) bundle, which is then routed to a spectrograph (SPEX 270M, Jobin-Yvon) for analysis. An intensified charge coupled device (ICCD) camera PIMAX-4 (Princeton Instrument), synchronized with the pump and probe lasers detects the dispersed white light from the spectrograph. The spectrograph records both the reference and sample spectra at the same time. Using Equation (1), the difference absorption spectra, *pump on* and *pump off* can be recorded by varying the delay time between pump and probe:

$$\Delta A = \log_{10} \left(\frac{s_{ref}^p}{s_{ref}^0} \times \frac{s_{sample}^0}{s_{sample}^p} \right) \quad (1)$$

where s_{ref}^p and s_{ref}^0 are reference spectra when the pump is on and off, respectively, while s_{sample}^p and s_{sample}^0 are sample spectra when the pump is on and off, respectively. All measurements were taken with a quartz cuvette of 10 mm x 10 mm dimension.

f. Electrochemical measurements

Cyclic voltammetric (CV) experiments were performed with a compact PalmSens4 driven by a computer using PSTrace software. Measurements were performed at room temperature in a single-compartment micro-cell. A glassy carbon (GC) electrode with a diameter of 2 mm was used as the working electrode. The auxiliary electrode was a Pt plate, and potentials are quoted against an Ag wire as reference electrode. All potentials are quoted relative to the ferrocene/ferrocenium internal standard. Electrochemical experiments were carried out in water-free, de-aerated acetonitrile with TBA.PF₆ (0.1 M) serving as a supporting electrolyte. Prior to the experimental runs, all solutions were purged with argon for at least 10 min to eliminate O₂, and they were maintained under a positive argon pressure throughout the experiment. The relevant potentials determined by the CVs were used to carry out chronoamperometry in the same three-electrode cell system described above (Preparation of samples). Using controlled potential coulometry method,¹⁰ the samples were quantitatively oxidized/reduced in an stepwise manner. Linear scan voltammetry (rotating disk electrode) measurements were recorded at

each coulometric step (before and after reduction) to ensure 100% reduction / oxidation process. The solutions containing reduced POMs were then analyzed with the help of Perkin Elmer Lambda 750 UV-Vis-NIR spectrophotometer.

2. Supporting data

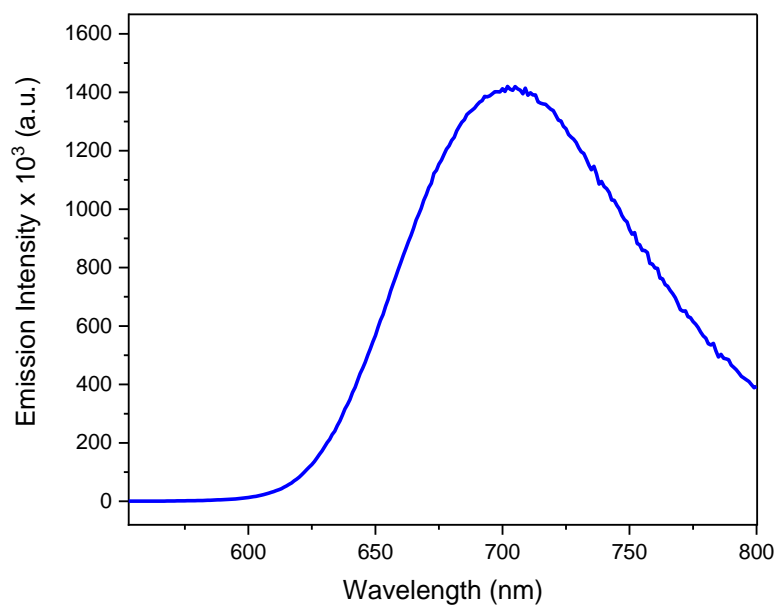


Figure S1. Emission spectrum of [Mo₆I₈Cl₆]²⁻ in deaerated acetonitrile, $\lambda_{\text{exc}} = 420$ nm

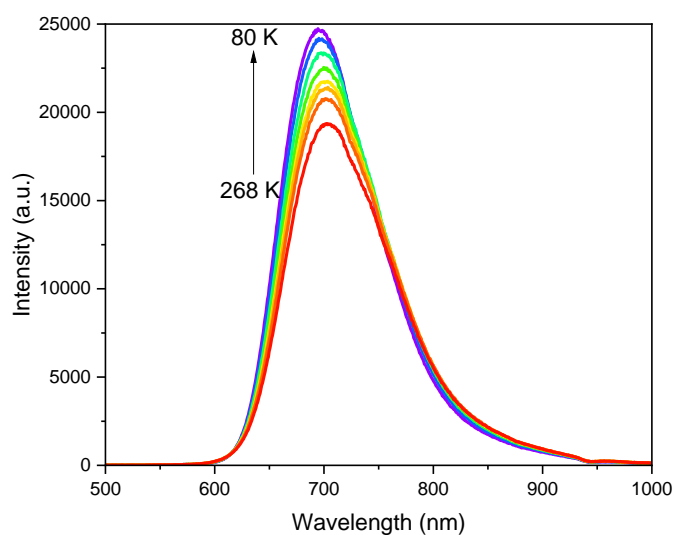


Figure S2. Emission spectra of [Mo₆I₈Cl₆]²⁻ powder at different temperatures from 268 to 80 K, $\lambda_{\text{exc}} = 375$ nm

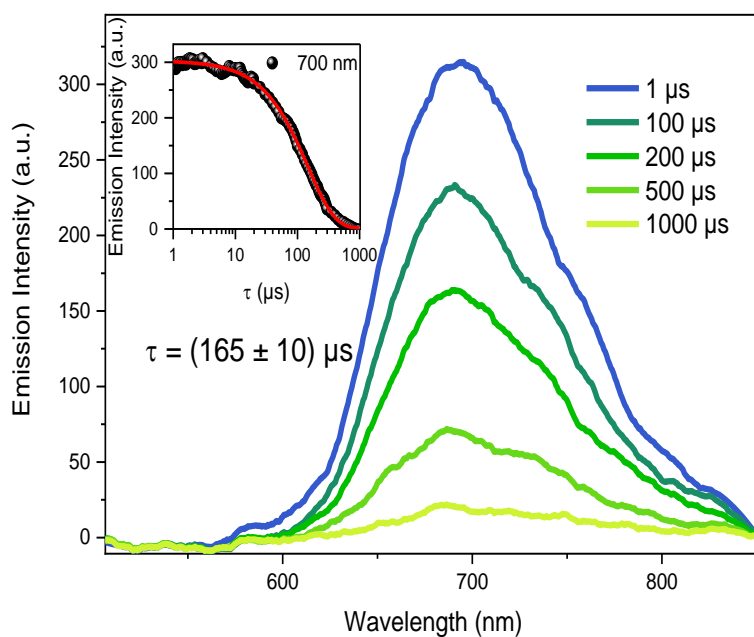


Figure S3. Time-resolved emission spectra of $[\text{Mo}_6\text{I}_8\text{Cl}_6]^{2-}$ detailed at indicated delay times ($\lambda_{\text{exc}} = 420 \text{ nm}$, 20 mW) in deaerated acetonitrile. The inset shows the monoexponential fit of the kinetics at the maximum of the emission

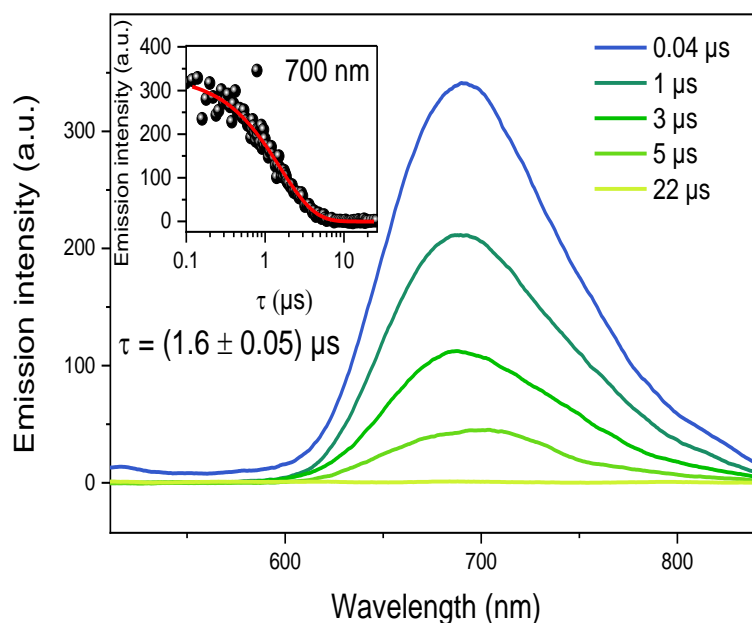


Figure S4. Time-resolved emission spectra detailed of $[\text{Mo}_6\text{I}_8\text{Cl}_6]^{2-}$ at different delays between pump ($\lambda_{\text{exc}} = 420 \text{ nm}$, 20 mW) and probe in aerated acetonitrile. The inset shows the monoexponential fit of the kinetics at 700 nm

Stern-Volmer (SV) plots were constructed to assess the Stern-Volmer constants (k_{sv}), according to the well-noted relationship: $\tau_0/\tau = 1 + k_{sv}[Q]$ or $I_0/I = 1 + k_{sv}[Q]$, where τ_0 and I_0 are emission lifetime and intensity in the absence of quencher respectively and $[Q]$ is quencher concentration. Finally, the quenching constants (k_q) were determined using $k_q = k_{sv}/\tau_0$.

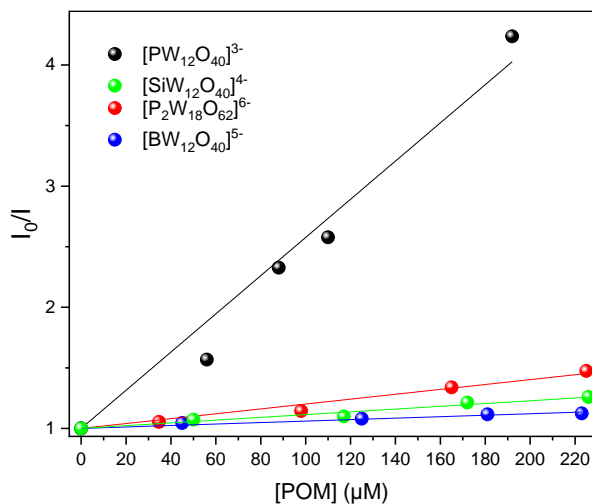


Figure S5. Stern-Volmer plots comparing the quenching efficiencies of the four POMs under study obtained from emission intensity of TBA₂[Mo₆I₈Cl₆] cluster excited state in deaerated acetonitrile

	$k_q \times 10^7, M^{-1} \cdot s^{-1}$
[PW ₁₂ O ₄₀] ³⁻	11 ± 2
[SiW ₁₂ O ₄₀] ⁴⁻	0.8 ± 0.2
[P ₂ W ₁₈ O ₆₂] ⁶⁻	1.4 ± 0.2
[PW ₁₁ VO ₄₀] ⁴⁻	1.5 ± 0.2
[SiW ₁₁ MoO ₄₀] ⁴⁻	1.9 ± 0.2
[SiMo ₁₂ O ₄₀] ⁴⁻	2.6 ± 0.5
[BW ₁₂ O ₄₀] ⁵⁻	0.5 ± 0.1
[H ₂ W ₁₂ O ₄₀] ⁶⁻	--

Table S1. Summary of emission quenching rate constants (k_q) obtained by the Stern-Volmer analysis of the emission intensities in the presence of different POMs.

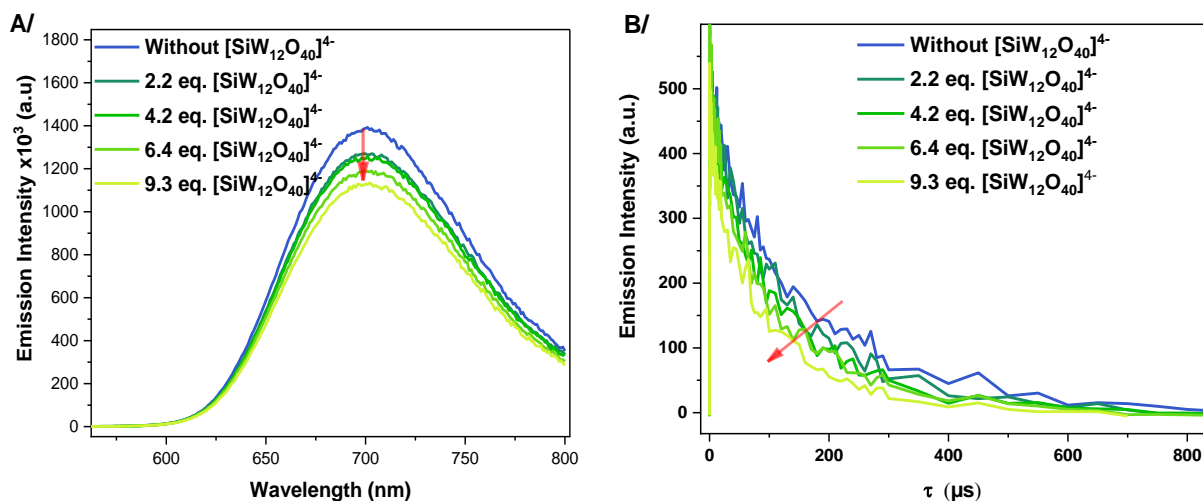


Figure S6. (A) Steady state emission spectra (corrected for POM absorption), and (B) time resolved emission decays of $[\text{Mo}_6\text{I}_8\text{Cl}_6]^{2-}$ - $[\text{SiW}_{12}\text{O}_{40}]^{4-}$ pair showing quenching of the cluster in deaerated acetonitrile, $\lambda_{\text{exc}} = 420 \text{ nm}$

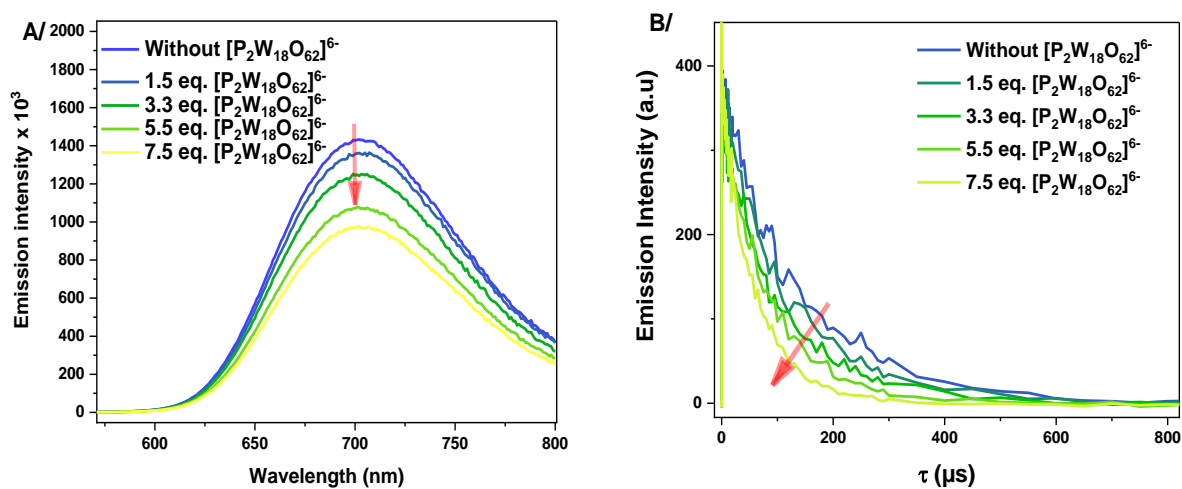


Figure S7. (A) Steady state emission spectra (corrected for POM absorption), and (B) time resolved emission decays of $[\text{Mo}_6\text{I}_8\text{Cl}_6]^{2-}$ - $[\text{P}_2\text{W}_{18}\text{O}_{62}]^{6-}$ pair showing quenching of the cluster in deaerated acetonitrile, $\lambda_{\text{exc}} = 420 \text{ nm}$

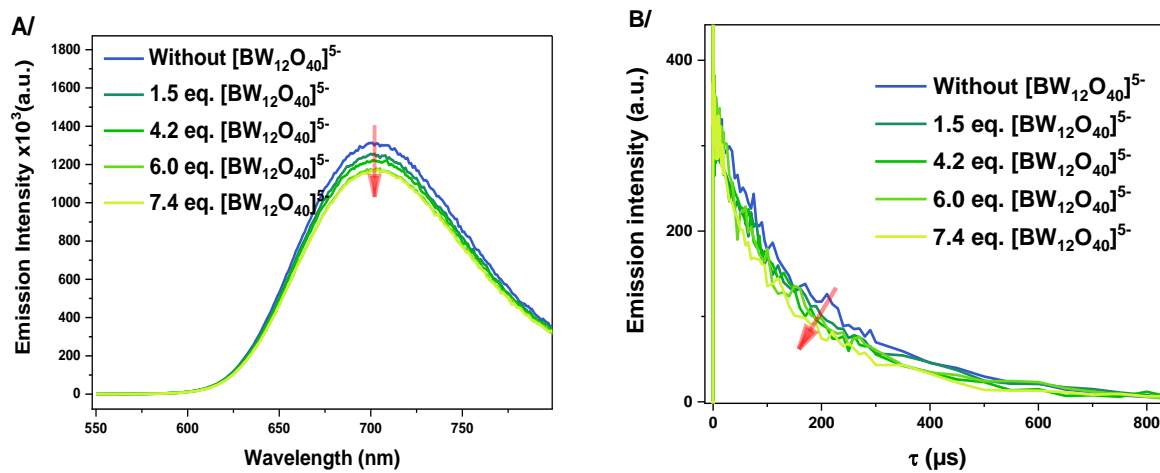


Figure S8. (A) Steady state emission spectra (corrected for POM absorption), and (B) time resolved emission decays of $[\text{Mo}_6\text{l}_8\text{Cl}_6]^{2-}$ - $[\text{BW}_{12}\text{O}_{40}]^{5-}$ pair showing quenching of the cluster in deaerated acetonitrile, $\lambda_{\text{exc}} = 420 \text{ nm}$

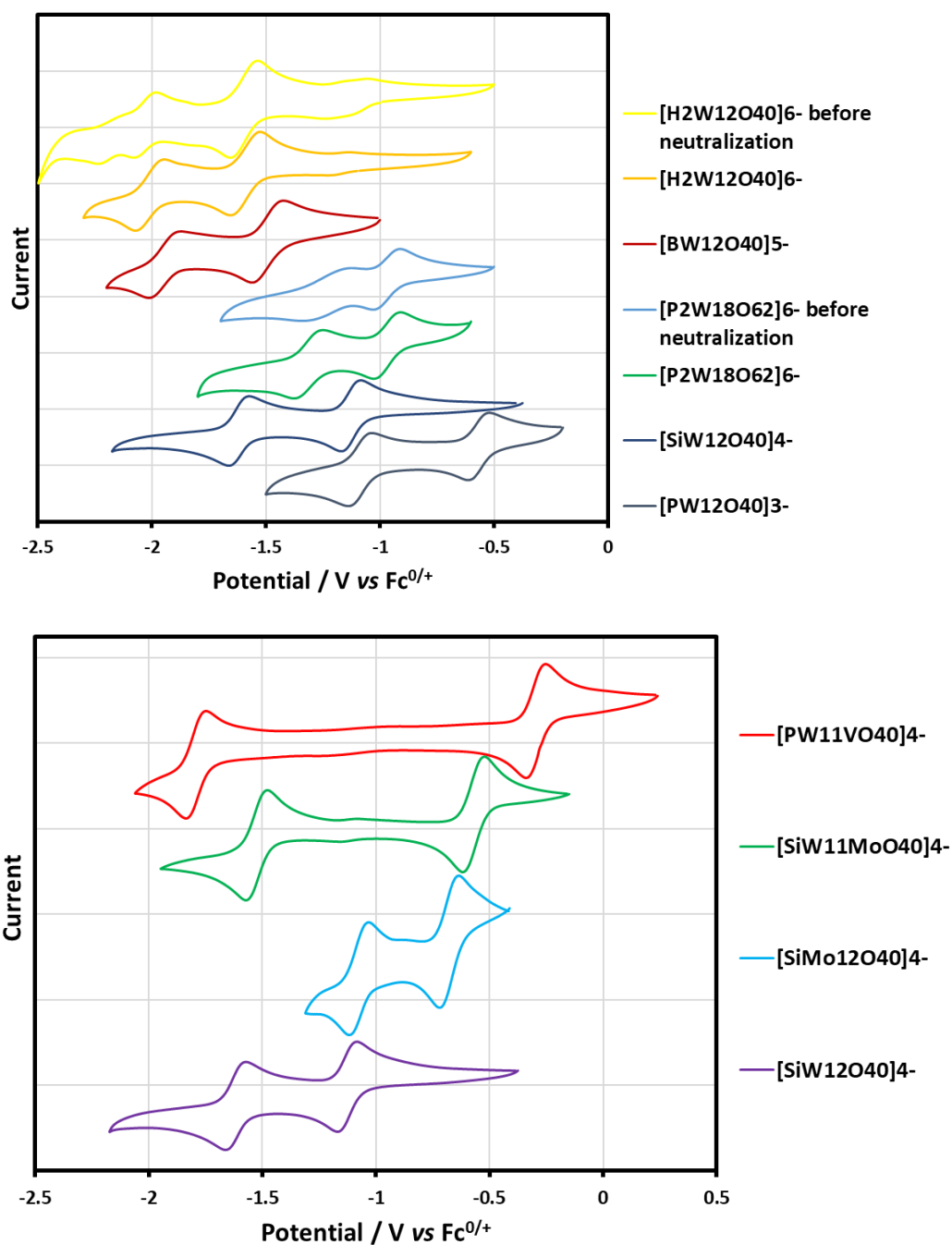


Figure S9. (TOP) Cyclic voltammograms of polyoxotungstate anions in anhydrous and deaerated acetonitrile with 0.1 M TBA.PF₆. Reference electrode: Ag wire; Working electrode: glassy carbon; and Auxiliary electrode: Carbon. The TBA salts of POMs ([H₂W₁₂O₄₀]⁶⁻ [P₂W₁₈O₆₂]⁶⁻) showed distorted ill-defined waves in CH₃CN due to the presence of protons. On the addition of about 1 eq. of TBA.OH per POM, the ill-defined waves disappeared completely, leaving a two-step redox wave. (BOTTOM) Cyclic voltammograms of isocharged POMs in anhydrous and deaerated acetonitrile with 0.1 M TBA.PF₆. Reference electrode: Ag wire; Working electrode: glassy carbon; and Auxiliary electrode: Carbon.

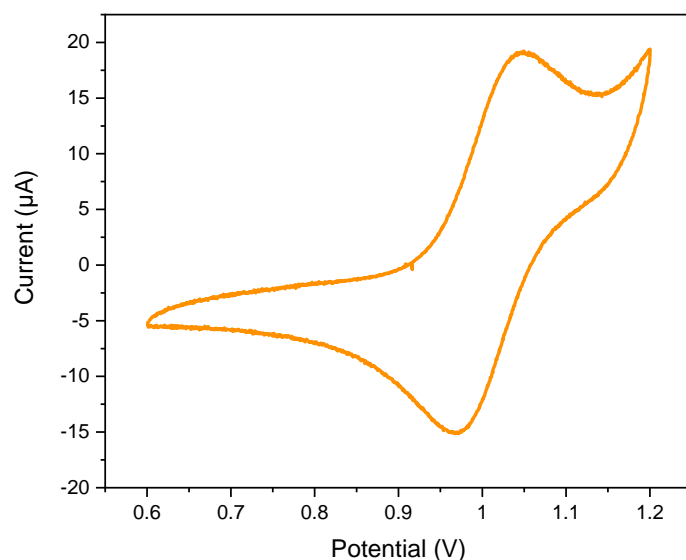


Figure S10. Cyclic voltammograms of $[\text{Mo}_6\text{I}_8\text{Cl}_6]^{2-}$ in deoxygenated water with 2 eq. of cyclodextrin. Reference electrode: Ag/AgCl (3M); Working electrode: glassy carbon; and Auxiliary electrode: Carbon.

It must be noted that the oxidation potential of the cluster $[\text{Mo}_6\text{I}_8\text{Cl}_6]^{2-}$ in organic solvent was found to be 0.6 V vs. Fc^+/Fc (see Dalton Trans., **2018**, 47, 1131). Therefore, the triplet state energy was estimated from the mean value of emission maxima to be higher than 1.78 eV. The oxidation potential of the triplet-excited state was then calculated to be lower than -1.18 V. Thus, the excited cluster is able to reduce most of the POM under study.

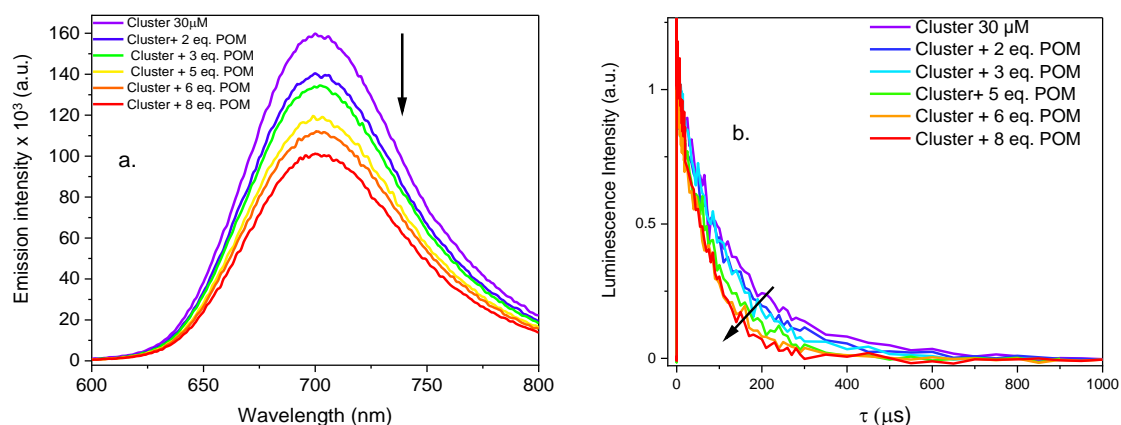


Figure S11. (a) Steady-state and (b) time-resolved emission quenching of the cluster by $[\text{PW}_{11}\text{VO}_{40}]^{4-}$ in deaerated acetonitrile, $\lambda_{\text{exc}} = 420 \text{ nm}$.

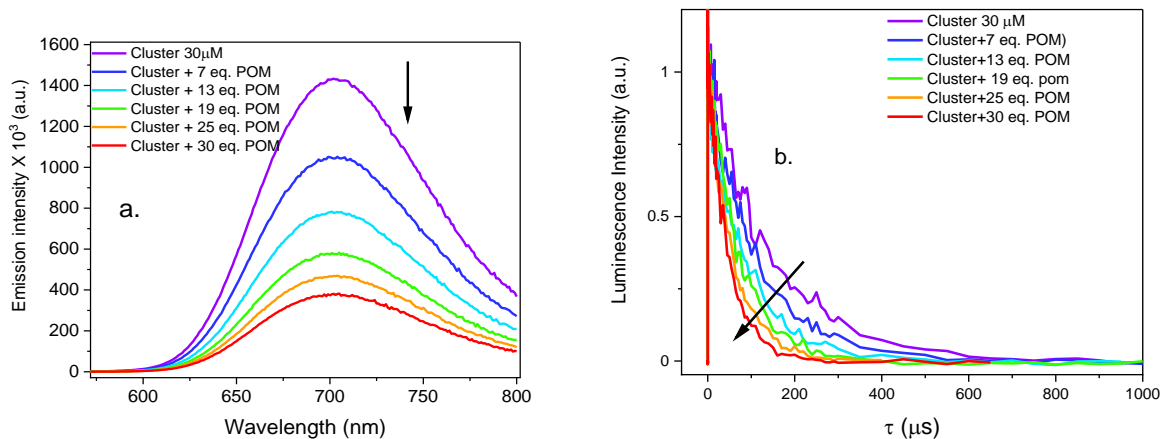


Figure S12. (a) Steady-state and (b) time-resolved emission quenching of the cluster by $[\text{SiW}_{11}\text{MoO}_{40}]^{4-}$ in deaerated acetonitrile, $\lambda_{\text{exc}} = 420 \text{ nm}$.

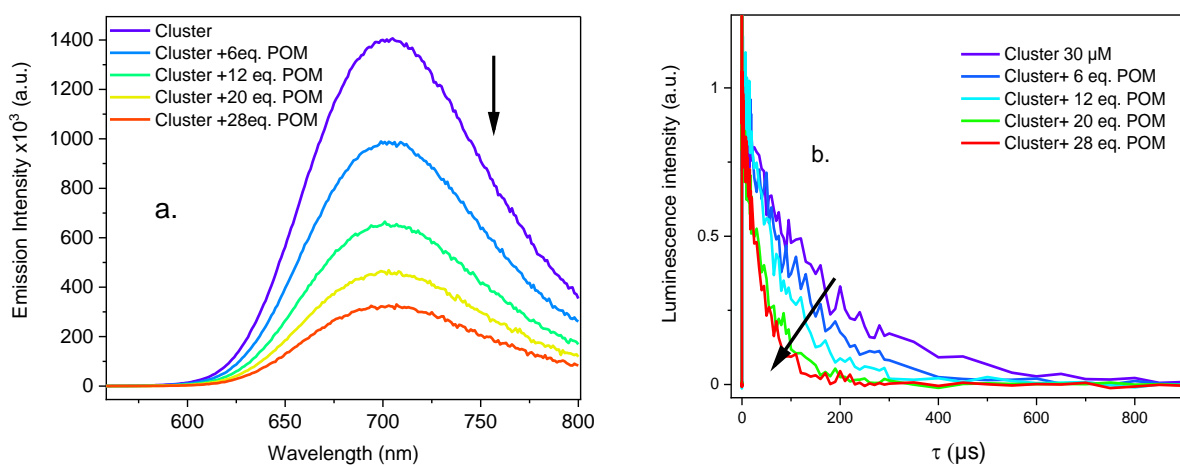


Figure S13. (a) Steady-state and (b) time-resolved emission quenching of the cluster by $[\text{SiMo}_{12}\text{O}_{40}]^{4-}$ in deaerated acetonitrile, $\lambda_{\text{exc}} = 420 \text{ nm}$.

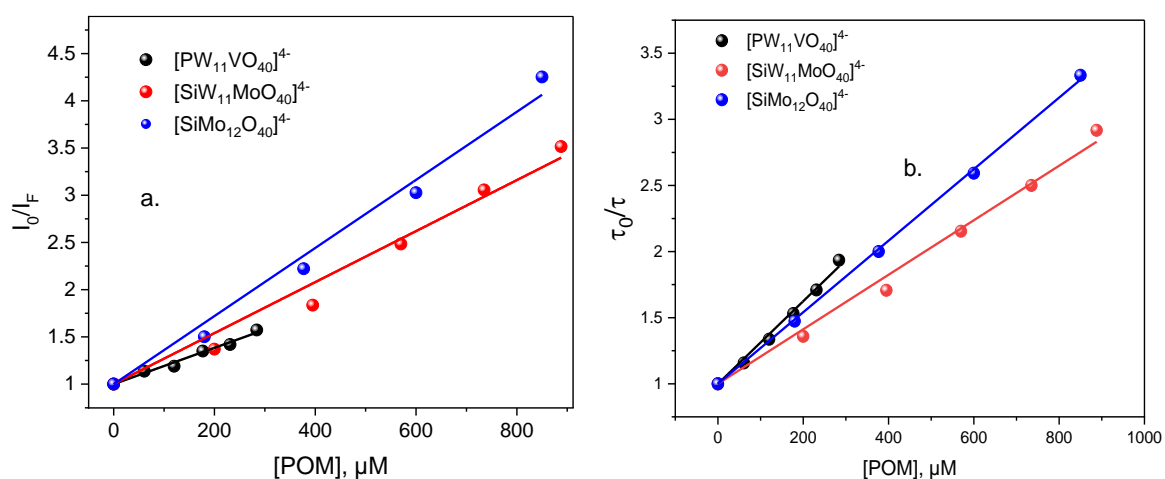


Figure S14. (a) Emission intensity and (b) lifetime Stern-Volmer plots for the three cluster-POM pairs.

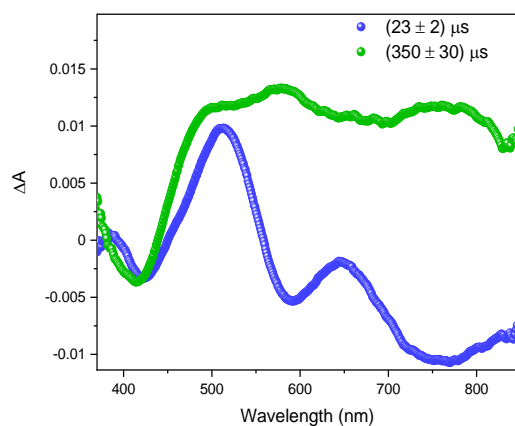


Figure S15. Decay associated difference spectra (DADS) of cluster- $[\text{PW}_{12}\text{O}_{40}]^{3-}$ obtained by global fitting of TA kinetics

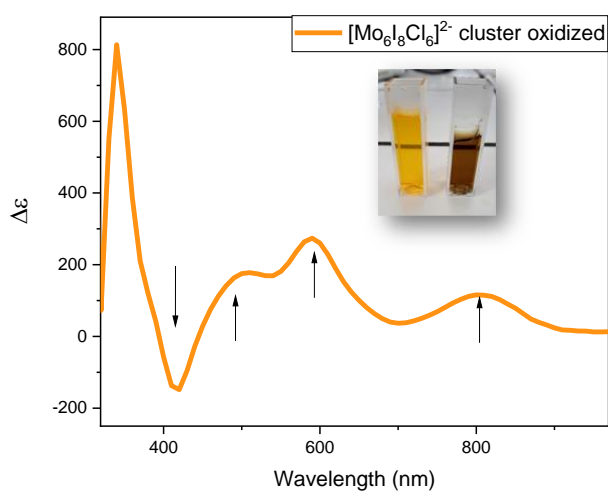


Figure S16. Spectro-electrochemical difference spectra of quantitatively oxidized molybdenum halide cluster

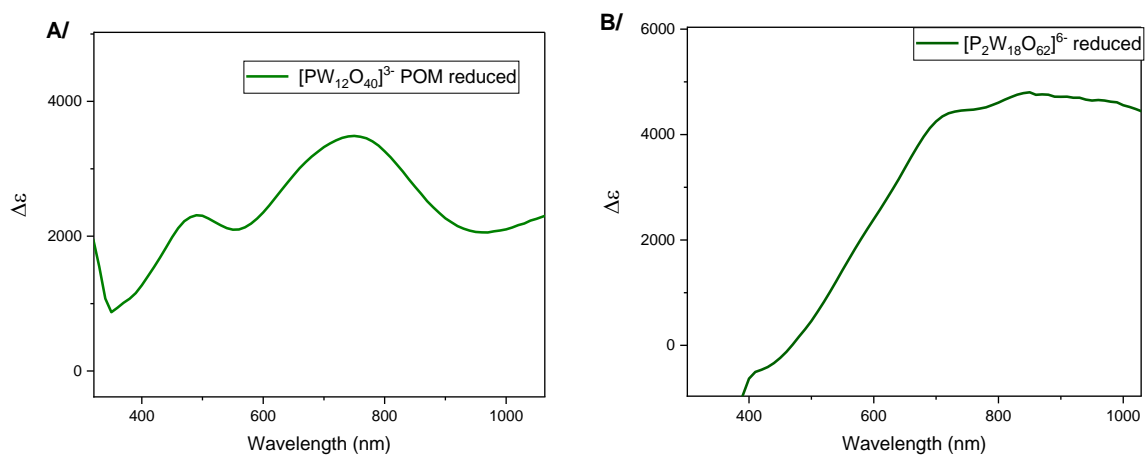


Figure S17. Spectro-electrochemical difference spectra of quantitatively one-electron reduced polyoxometalate anions (A) $[\text{PW}_{12}\text{O}_{40}]^{3-}$, and (B) $[\text{P}_2\text{W}_{18}\text{O}_{62}]^{6-}$ in acetonitrile

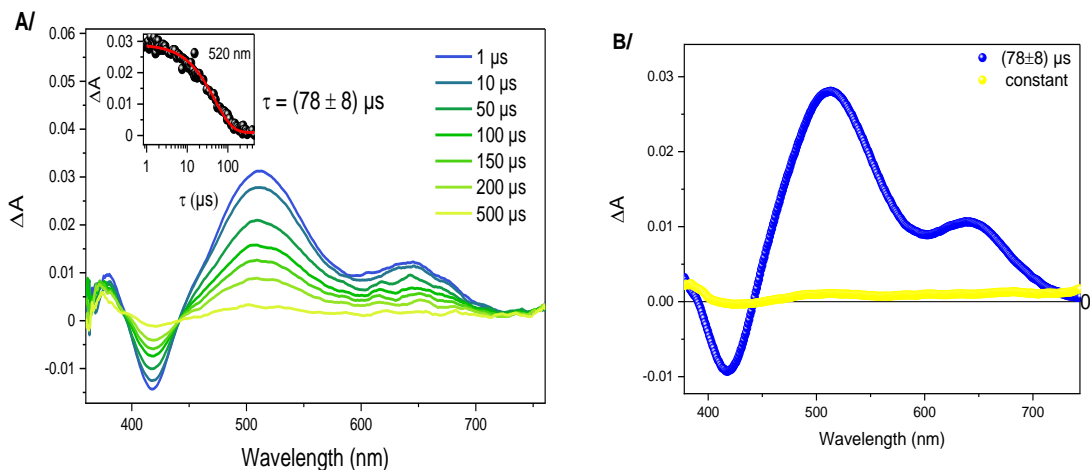


Figure S18. (A) TA spectra along with the kinetic fit at 520 nm shown in the inset and (B) decay associated difference spectra (DADS) of cluster (60 μM)-[BW₁₂O₄₀]⁵⁻ (300 μM) POM pair obtained by global fitting of TA kinetics ($\lambda_{\text{exc}} = 420 \text{ nm}$, 20 mW).

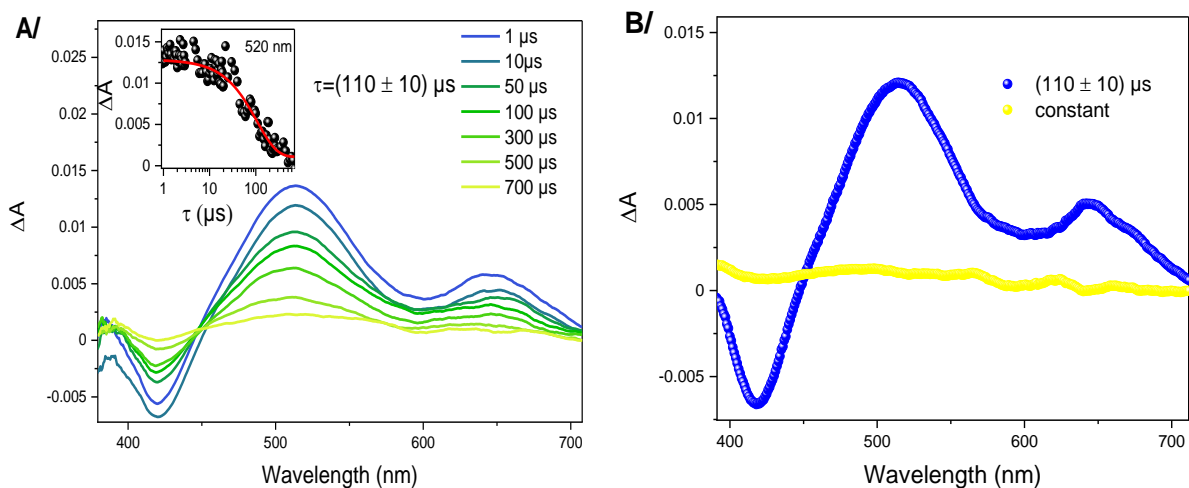


Figure S19. (A) TA spectra along with the kinetic fit at 520 nm shown in the inset and (B) decay associated difference spectra (DADS) of cluster (60 μM)-[H₂W₁₂O₄₀]⁶⁻ (300 μM) POM pair obtained by global fitting of TA kinetics ($\lambda_{\text{exc}} = 420 \text{ nm}$, 20 mW)

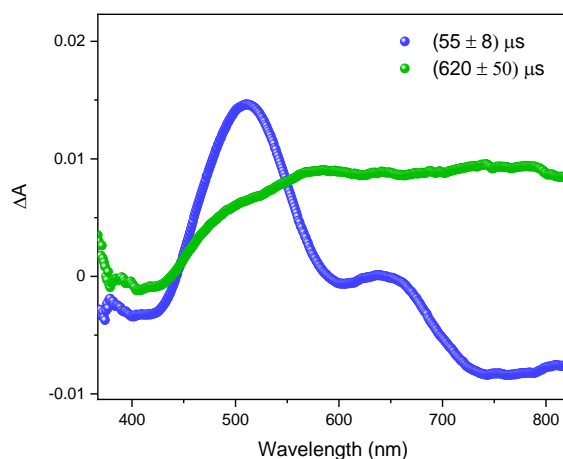


Figure S20. Decay associated difference spectra (DADS) of cluster- $[P_2W_{18}O_{62}]^{6-}$ POM pair obtained by global fitting of TA kinetics

3. Author contributions

Conceptualization: CF, EC, RM, MHHT; investigation: AF, YS, CF, NL, YM, MH, EC, SC, TP, CD, MHHT; supervision: CF, RM, KS, MHHT; writing—original draft preparation: AF, CF, MHHT; funding acquisition: CF, EC, MHHT, RM, TP. All authors have reviewed and agreed to the submitted version of the manuscript.

4. References

- 1 N. A. Vorotnikova, Y. A. Vorotnikov, I. N. Novozhilov, M. M. Syrovkashin, V. A. Nadolinny, N. V. Kuratieva, D. M. Benoit, Y. V. Mironov, R. I. Walton, G. J. Clarkson, N. Kitamura, A. J. Sutherland, M. A. Shestopalov and O. A. Efremova, *Inorg. Chem.*, 2018, **57**, 811–820.
- 2 C. Falaise, A. A. Ivanov, Y. Molard, M. A. Cortes, M. A. Shestopalov, M. Haouas, E. Cadot and S. Cordier, *Mater. Horizons*, 2020, **7**, 2399–2406.
- 3 S. Yao, C. Falaise, A. A. Ivanov, N. Leclerc, M. Hohenschutz, M. Haouas, D. Landy, M. A. Shestopalov, P. Bauduin and E. Cadot, *Inorg. Chem. Front.*, 2021, **8**, 12–25.
- 4 H. Wu, *J. Biol. Chem.*, 1920, **43**, 189–220.
- 5 C. Rocchiccioli-Deltcheff, M. Fournier, R. Franck and R. Thouvenot, *Inorg. Chem.*, 1983, **22**, 207–216.
- 6 I.-M. Mbomekallé, Y. W. Lu, B. Keita and L. Nadjo, *Inorg. Chem. Commun.*, 2004, **7**, 86–90.
- 7 A. Téazé, G. Hervé, R. G. Finke and D. K. Lyon, in *Inorganic Syntheses*, John Wiley & Sons, Ltd, 1990, pp. 85–96.
- 8 C. Sanchez, J. Livage, J. P. Launay, M. Fournier and Y. Jeannin, *J. Am. Chem. Soc.*, 1982, **104**, 3194–3202.
- 9 A. A. Ivanov, M. Haouas, D. V. Evtushok, T. N. Pozmogova, T. S. Golubeva, Y. Molard, S. Cordier, C. Falaise, E. Cadot and M. A. Shestopalov, *Inorg. Chem.*, 2022, **61**, 14462–14469.
- 10 J. E. Harrar, *Trends Anal. Chem.*, 1987, **6**, 152–157.